Cirrus cloud radiative effect on surface-level shortwave and longwave irradiances at regional and global scale

J-C. Dupont [(1)], M. Haeffelin [(1)], C. N. Long [(2)]

(1) Institut Pierre-Simon Laplace, Paris, France
(2) Pacific Northwest National Laboratory, Richland, WA, USA

jean-charles.dupont@lmd.polytechnique.fr /Fax: +33169335108 / Phone: +33169335145

ABSTRACT

In this study, we analyze two datasets: ground-based and satellite measurements. The firsts corresponds to solar and infrared irradiance measurements, cloud and aerosol Lidar backscattering profiles, microwave radiometer brightness temperatures, radiosonde profiles, and sun-photometer extinctions monitored at four observatories located in the midlatitudes, the Tropics and the Arctic. This dataset permits to estimate the Cirrus cloud Radiative Forcing on surface-level shortwave (CRE_{SW}) and longwave (CRE_{LW}) irradiances. The sensitivity of CRE_{SW} to Cloud Optical Thickness (noted CRE_{SW}*) is established and ranges from 100 W m^{-2} to 200 W m^{-2} per unit of cloud optical thickness. The important variability of aerosols and water vapor content obtained in studying the 4 observatories allows us to quantify the combined influence of aerosol optical thickness and integrated water vapor on CRESW* : 10 to 20 % CRE_{SW}* range for turbid and pristine atmosphere. Moreover, the sensitivity of the CRFLW to both cloud emissivity and cloud temperature (noted CRE_{SW}*) is established and the influence of integrated water vapor on CRE_{LW}* quantified. The long-term dataset allows quantifying the impact of subvisible cirrus cloud on the anomaly of direct and diffuse solar irradiances at the surface over ARM SGP site since 10 years.

Satellite measurements are used next as input parameters to the cirrus cloud radiative forcing parameterizations to calculate CRE_{SW} and CRE_{LW} at global scale. CALIOP provide aerosol and cirrus cloud properties and AIRS the integrated water vapor. Meridian distribution are shown and discussed. They reveal a positive cirrus cloud net radiative effect (CRE_{SW} + CRE_{LW}) from 30°N poleward during boreal winter and from 45°S during austral winter. The cumulative cirrus cloud net radiative effect reaches +1.5 W m^{-2} for these two winter cases and -8 W m^{-2} near the equator.

1. INTRODUCTION

Numerous studies have demonstrated that the global average frequency of cirrus cloud occurrence is near 17% ([1]) and can reach 45% in the Tropics with a maximum occurrence frequency up to 70% near the tropics over the 100°–180°E longitude band ([2]). The significant coverage of cirrus clouds, their persistence, their large area extent and their high altitude make them important components in the total radiation budget and in the vertical transport of energy through radiative processes ([3]). Reference [4] has identified that these clouds are one of the sources of uncertainty in the study of Earth's radiation budget and climate.

To precisely quantify the surface CRE and to understand the relationship between this CRE and cloud / atmospheric properties, accurate measurements of each parameter added to simultaneously radiation measurements have to be taken. Reference [5] shows that the predominant surface CRE are associated with thin cirrus cloud layers and thick low-level clouds, due in part to their very frequent occurrence compared to other types of clouds. Reference [6] establishes correlations between cloud fraction and surface CRE and quantify the seasonal cycle of CRE showing an average annual CRE_{SW} (CRE_{LW}) of -37 W m^{-2} (17 W m^{-2}) for high altitude clouds. Finally, reference [7] quantifies the relationship between CRE and cirrus cloud and atmospheric properties. CRE_{SW} (CRE_{LW}) is driven by cloud optical thickness and atmospheric turbidity (water vapor amount and cirrus infrared emissive power).

In this study, we present (1) the correlations between CRE and macrophysical and optical properties of cirrus cloud modulated by atmospheric compositions, (2) the monthly CRE_{SW} and CRE_{LW} cycle for continental, arctic, tropical and oceanic sites and (3) the global distribution of surface CRE induced by cirrus cloud for 2006-2007 periods.

2. OBSERVATIONAL DATA SETS

2.1 Ground-based measurement

To quantify the high altitude cloud radiative forcing at the surface, we need the following informations: (1) high quality shortwave and longwave irradiance measurements, (2) screen-level temperature and water-vapor pressure, (3) column-integrated water vapor density and aerosol optical thickness, (4) vertical profiles of temperature, and finally (5) unambiguous identification of cloud-free and cloudy situations. We choose to use measurements from two mid-latitude sites, the SIRTA Observatory and the ARM SGP Lamont site, one tropical site with the ARM TWP Nauru site and finally one arctic site with ARM NSA Barrow site.

These four multi-latitude sites are characterized by different climate regimes like US continental for Lamont, French oceanic/sub-urban for SIRTA, coastal tropical and arctic for Nauru and Barrow respectively. The variability in terms of aerosols, water vapor and clouds is very large between each site and permit to study the impact of this very important range of atmospheric and high altitude cloud properties on shortwave and longwave irradiances received at the surface (Figure 1).

© Proceedings of the 8th International Symposium on Tropospheric Profiling, ISBN 978-90-6960-233-2
Delft, The Netherlands, October 2009. Editors, A. Apituley, H.W.J. Russchenberg, W.A.A. Monna

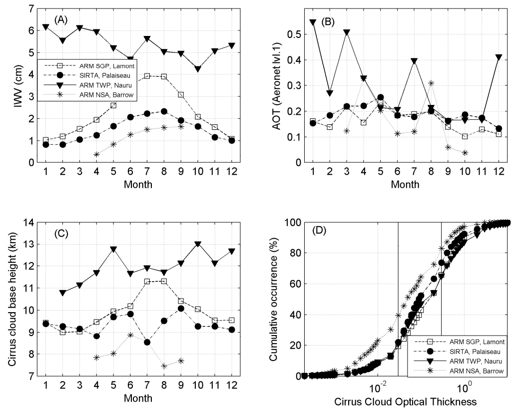

Figure 1. *Monthly mean integrated water vapor (A), aerosol optical thickness (B) and cirrus cloud base altitude (C) for each site. Figure 1D is the cumulative distribution of the cirrus cloud optical thickness. Black triangles correspond to ARM TWP Nauru site, white squares to ARM SGP Lamont site, black dots to SIRTA Palaiseau site and black stars to ARM NSA Barrow site.*

2.2 Spatial observations data set

Cirrus cloud and aerosol properties at global scale are here obtained in using observations from the Cloud-Aerosol Lidar with Orthogonal Polarization (CALIOP) spaceborne lidar, part of the CALIPSO mission ([8]). The CALIPSO satellite was launched in April of 2006 and passes in the same track every 16 days [9]. Official CALIOP Level 2 (version 2) data products are used in this study [9]. We use 1 year of CALIOP data products in the 2006/07-2008/06 period to sample all seasons uniformly. Both daytime and nighttime data are considered.

Water vapor content at global scale is collected from the observations provided by The Atmospheric Infrared Sounder (AIRS). AIRS was launched on the Aqua research satellite, a major component of NASA's Earth Observing System, in May 2002. Integrated water vapor level 2 version 5 data products are used in this study.

2.3 Clear-sky and overcast period detection

In this study, the term "clear-sky" is defined as a sky without any liquid water or ice cloud. Clear-sky periods during daytime are selected by two automated methods r based on shortwave and longwave irradiances. However, this methodology can be biased by optically-thin clouds [10]. Hence, to be sure of the totally clear-sky situations, we add a threshold algorithm based on lidar measurements.

Observed periods are defined as overcast when all lidar profiles within 1-hour contain clouds. Only clouds with base altitude higher than 7 km are here considered with no cloud below for SGPA, SIRTA and TWP site. Concerning NSA site we consider all clouds higher than 4 km in order not to consider only Polar Stratospheric Clouds Additionally, only overcast periods longer than 3 hours are considered to ensure a persistent impact on LW and SW irradiances.

3. SENSITIVITY OF CIRRUS RADIATIVE EFFECT

Cirrus cloud radiative effect estimations require precise references of solar and infrared irradiances for the cloud-free atmosphere. In fact, the cirrus cloud radiative effects at the surface on both shortwave (CRE_{SW}) and longwave irradiances (CRE_{SLW}) are defined as the difference between the shortwave and longwave irradiances measured in overcast situations and the clear-sky references values. In this study, clear-sky reference values are obtained from parameterizations fitted directly to observed data.

3.1 Shortwave radiative effect parameterization

Figure 2 shows a scatter plot of the shortwave cirrus cloud radiative effect (CRE_{SW}) versus COT for all the dataset that correspond to almost 5100 15-min periods. The dotted black line is the best linear fit optimized by the method of the least squares applied on the CRE_{SW} median every 0.1 COT step. The black dot markers correspond to CRE_{SW} median every 0.1 COT step. The slope of this fit is –118 W m^{-2} COT^{-1} with a correlation factor of 0.81.

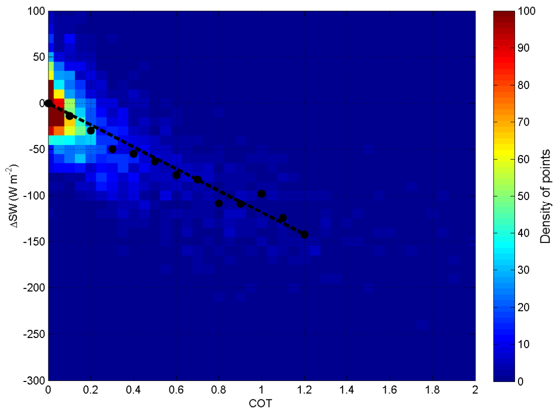

Figure 2. *Scatter plot of the shortwave cirrus cloud effect (CRESW) versus COT for the data collected in all the sites. The dashed line is the best linear fit optimized by the method of the least squares applied on the CRESW median every 0.1 COT step. The dot markers correspond to the CRESW median every 0.1 COT step.*

The cirrus cloud effects on surface solar irradiance can also be modulated by the solar illumination geometry, here represented by the solar zenith angle (SZA). The relative contribution of the diffuse irradiance to the total shortwave increases with the solar zenith angle (see equation 1).

Aerosol and water vapor located between the ground surface and the cirrus cloud base can also modulated the cirrus cloud effects on surface solar irradiance. To quantify these variables, we consider the combined effect of aerosol and water vapor rather than each independently parameter. We also use the aerosol optical thickness (AOT) and the water vapor optical thickness (WVOT).

Equation 1 illustrates the different equations taking into account these variables necessary to quantify as precisely as possible the CRE_{SW} every 15-min period over each site.

$$
\begin{aligned}
&CRE_{SW} = CRE_{SW}* \times COT \\
&and \quad CRE_{SW}* = P_{(cSZA)} + P_{1(AOT+WVOT)} \\
&\quad with \quad P_{(cSZA)} = -222.1 \times cSZA^3 + 480.7 \times cSZA^2 - 358.0 \times cSZA - 36.6 \\
&\quad and \quad P_{1(AOT+WVOT)} = -166.1 \times (AOT + WVOT) + 44.2
\end{aligned}
$$

(1)

3.2 Longwave radiative effect parameterization

The longwave irradiance emitted by the cirrus cloud is noted LW_{cirrus} and is computed from Stephan-Boltzmann's law based on the cirrus cloud infrared emissivity and thermodynamic temperature inside the cirrus cloud. The cloud thermodynamic temperature is derived by combining radiosonde and Lidar measurements that provide temperature profiles and cloud mean altitude, respectively. Temperatures are interpolated between radiosoundings at the time and altitude of lidar observations.

As water vapor is an efficient absorber of longwave radiation and water vapor content is highly variable on synoptic and seasonal scales, measured CRE_{LW} is likely to be affected by the water vapor content of the atmosphere between surface and cloud base. For a totally dry atmosphere or totally wet atmosphere, CRF_{LW}* is 0.32 or 0.02 respectively.

Equation 2 sums up de methodology used to quantify de cirrus cloud effect on longwave irradiance measured at the surface. We present the definition of the CRE_{LW}*, the parametric equation associated with and the γ term used in the calculation.

$$
\begin{aligned}
&CRE_{LW} = CRE_{LW}* \times LW_{cirrus} \\
&and \quad CRE_{LW}* = -0.13 \times \gamma^3 + 0.51 \times \gamma^2 - 0.63 \times \gamma + 0.32 \\
&with \quad \gamma = \frac{\varepsilon \times \left(e/T\right)^2}{IWV} \times 10000
\end{aligned}
$$

(2)

4. INSTANTANEOUS AND CUMULATIVE CRE

The relative importance of the cirrus clouds in the current climate's radiation budget also depends on their abundance. In fact, as shown by [11] the cloud fraction of the cirrus cloud induced a cumulative SW (LW) cloud effect stronger than low level-clouds. We define the sunshine duration ratio as the ratio between sunshine duration period in hours and 24. Hence, the cumulative cirrus cloud effect equals the instantaneous CRE_{SW} (CRE_{LW}) multiplies by the cloud fraction and the sunshine duration ratio (we calculate a day and night CRE_{LW}).

4.1 Monthly variations at regional scale

The monthly means of the LW, SW, and NET cirrus cloud instantaneous radiative effect for SGP, SIRTA and TWP sites are illustrated in Figure 3. CRE_{NET}, the sum of SW and LW cirrus cloud radiative effect, are primarily determined by CRE_{SW} throughout most of the year. During winter, however, the negative CRE_{SW} and positive CRE_{LW} nearly cancel each other, resulting in CRE_{NET} of -7 and -7.6 W m^{-2} for SIRTA and SGP sites. CRE_{LW} over SGP site has a significant annual cycle, due to the important range of water vapor (Figure 1) inducing important range of CRE_{LW}*, with value ranging between 18.3 W m^{-2} to 10.7 W m^{-2} in winter and summer respectively. CRE_{SW} is a little bit higher in summer period over SGP and SIRTA sites (+10-15 W m^{-2} of radiative impact during summer compared to winter period) in correlation with smaller solar zenith angle (synonymous of a higher CRF_{SW}*). Finally, we note a net positive impact in February (7 W m^{-2}) and near 0 W m^{-2} in March and December (-1.1 and -0.2 W m^{-2}) over SGP site and of 0.3 W m^{-2} in November over SIRTA site. Cirrus net effect over TWP site is mainly composed of the SW effect (seasonal average ranging from -49 to -16 W m^{-2}) because of the very limited LW effect (annual average of 1.0 W m^{-2}).

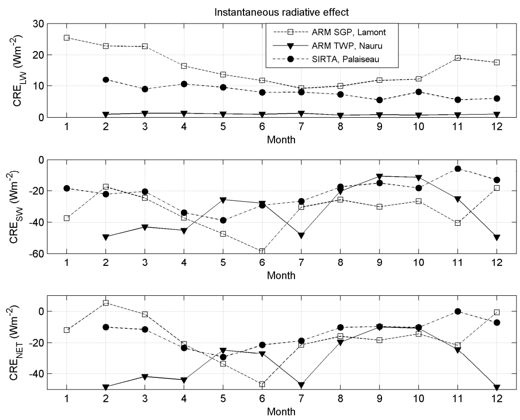

Figure 7: Monthly mean instantaneous cirrus cloud radiative effect on longwave, shortwave and net fluxes over ARM SGP, ARM TWP and SIRTA sites.

4.2 Seasonal and zonal variations at global scale

To calculate de cumulative cirrus cloud effect, we calculate for each 2.5°x2.5° the cloud fraction and the sun-shine duration. Cirrus cloud fraction (not shown here) reaches almost 60% near the equator, 30% for 30°N-60°N and 25% for 30°S-60°S.

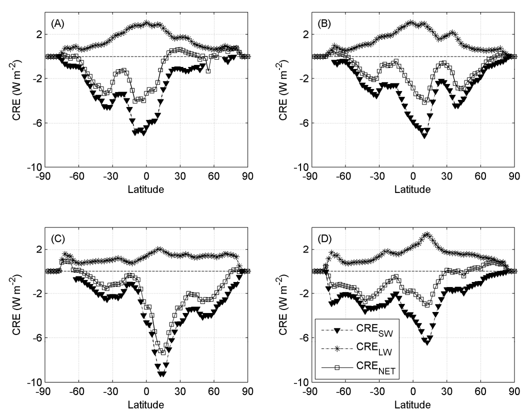

Figure 10. *Zonal cirrus cloud cumulative effect at the surface for the different seasons: (A) Winter, (B) Spring, (C) Summer and (D) Autumn. Black triangles correspond to shortwave cirrus cloud radiative effect, stars to the longwave radiative effect and squares to the net radiative effect at the surface.*

The global mean values of the cumulative CRE are -2.8, 1.7 and -1.1 W m^{-2} for CRE_{SW}, CRE_{LW} and CRE_{NET} respectively. Reference [11] showed an impact of -3.6, 1.1 and -2.5 W m^{-2}. Main differences come from the definition of the cumulative effect that they defined without account for the sunshine duration what tend to increase the CRE_{SW} and minimize the CRE_{LW}. The decreasing of the sunlight duration during the winter induces a net positive CRE starting from 20°N and 30°N for the autumn reaching a maximum of 0.8 W m^{-2}. The CRE_{LW} is maximum near the equator, with 1.5 W m^{-2}, due to the much more important cloud fraction that compensate the strong water content in this region. However, the net effect if negative in this region related to the strong CRE_{SW}. The seasonal average of CRE_{SW} is relatively constant for 15°S-15°N zone (average value of -5.2 W m-2) whereas the range is much more significant for 15°S-45°S (-4.1 W m^{-2} in winter and -2.0 W m^{-2} in summer) and for 15°N-45°N (-1.3 W m^{-2} in winter and -4.8 W m^{-2} in summer). This range is related to the ITCZ variability that induced important changes in the cirrus cloud fraction in North and South hemisphere.

5. CONCLUSIONS

In this study, we derive (1) the sensitivity of surface CRE_{SW} to the cloud optical thickness modulated by the solar zenith angle and the atmospheric turbidity (noted CRE_{SW}*) and (2) the sensitivity of surface CRELW to the infrared emissive power of cirrus cloud modulated by the water vapor content (noted CRE_{LW}*). The average CRE_{SW}* is -120 W m^{-2} COT^{-1} but it ranges from -80 to -140 m^{-2} COT^{-1} depending on the solar illumination with a residual variability ranges from + 40 and -40 W m^{-2} COT^{-1} from pristine to turbid conditions respectively. We have also established one parametric equation that accounts for this variability, considering solar zenith angle and water vapor and aerosol optical thickness as input parameter. The CRE_{LW}*, that corresponds to the infrared transmissivity of the atmosphere, ranges from 3% to 40% from dry to wet atmospheric conditions respectively and is also parameterized.

The four ground-based sites displayed significant differences concerning CRE_{SW} and CRE_{LW} annual average and the seasonal variability. The mid-latitude ARM SGP site presents a seasonal mean CRE_{LW} greatest during the winter (18 W m^{-2}) and least during summer (10 W m^{-2}) due to water vapor mask and annual cycle of cirrus cloud base altitude dependency. The tropical ARM TWP site displayed quasi-null CRE_{LW} with annual average value about 1 W m^{-2} related to strong water vapor content. The subvisible cirrus class (COT<0.03) over mid-latitude sites, that represents 20% of the population, induces a significant increase in surface LW irradiance at the 2-7 W m^{-2} level. The semi-transparent cirrus class (0.03<COT<0.3), that represents 45% of the population, will affect the surface SW irradiance by –12 to –25 W m^{-2}. The SW radiative impact of medium altitude cirrus clouds (9-11 km) is ranges from -20 to -45 W m^{-2}, while that of the thicker cirrus (0.3<COT<3) is greater than 95 W m^{-2} on average.

Global CRE estimations show very significant zonal and seasonal variability of each components of the CRE_{NET}. CRE_{NET} is 0.4 W m^{-2} during winter/autumn for 15°N-75°N and 1 W m-2 for 45°S-75°S whereas near -3 W m^{-2} for 15°S-15°N (major influence of the sunshine duration that modulate significantly the ratio CRE_{SW}/CRE_{LW}). Summer period shows a cirrus cloud global cooling at all the latitudes except for 75°S-45°S with a quasi null effect and a peak at -3.6 W m^{-2} for 15°S-45°N. The global average cumulative CRE are -2.8, 1.7 and -1.1 W m^{-2} for CRE_{SW}, CRE_{LW} and CRE_{NET} respectively. For high latitudes region (tropic), 45°N-75°N (15°S-15°N) these annual average values are -1.3, 0.9 and -0.4 W m^{-2} (-5.2, 2.4 and -2.8 W m^{-2}) respectively. These important zonal and seasonal CRE values highlight that cirrus clouds can affect significantly regional and global radiative budget and that we ought to optimize the parameterization taken into account in the climate modelling.

REFERENCES

[1] Dessler, A. E., and P. Yang, 2003: The distribution of tropical thin cirrus clouds inferred from Terra MODIS data*, J. Clim.*, **16**, 1241 – 1247

[2] Nazaryan, H., M. P. McCormick, and W. P. Menzel, 2008: Global characterization of cirrus clouds using CALIPSO data, *J. Geophys. Res.*, **113**

[3] Stephens, G. L., 2005: Cloud feedbacks in the climate system: A critical review, *J. Clim.*, **18**, 237– 273,

[4] Lynch, D., 2002: Cirrus: History and definitions, in Cirrus, edited by D. Lynch et al., 3-10, *Oxford Univ. Press*, New York.

[5] Mace G., S. Benson and S. Kato, 2006: Cloud radiative forcing at the Atmospheric Radiation Measurement Program Climate Research Facility: 2. Vertical redistribution of radiant energy by clouds, *Journal of Geophysical Research*, **111**,

[6] Dong X., Xi B., Minnis P., 2005: A Climatology of Midlatitude Clouds from the ARM SGP Central Facility. Part II: Cloud Fraction and Surface Radiative Forcing, *Journal of Climate,* **19**, 1765–1783.

[7] Dupont J-C., M. Haeffelin, 2008: Observed instantaneous cirrus radiative effect on surface level shortwave and longwave irradiances, *Journal of Geophysical Research*, 2008JD009838

[8] Winker, D. M., M. A. Vaughan, A. H. Omar, Y. Hu, K. A. Powell, Z. Liu, W. H. Hunt, and S. A. Young, 2009: Overview of the CALIPSO Mission and CALIOP Data Processing Algorithms, *J. Atmos. Oc. Technol.*

[9] Currey J. C., T. Tremas, D. M. Winker, J. Pelon et al., 2007: Cloud – Aerosol LIDAR Infrared Pathfinder Satellite Observations, Data Management System, Data Products Catalog, Document No: PC-SCI-503.

[10] Dupont J-C., M. Haeffelin and C. N. Long, 2008: Evaluation of cloudless-sky periods detected by shortwave and longwave algorithms using lidar measurements, Geophysical Research Letter, 2008GL033658

[11] Chen, T., W. B. Rossow, and Y. Zhang, 2000 : Radiative effects of cloud-type variations, *Journal of Climate*, **13**, 264–286.